PHYSICAL REVIEW D **94,** 115028 (2016)

Neutrino mass model with S_3 symmetry and seesaw interplay

Soumita Pramanick* and Amitava Raychaudhuri†

Department of Physics, University of Calcutta,
92 Acharya Prafulla Chandra Road, Kolkata 700009, India

(Received 14 November 2016; published 27 December 2016)

We develop a seesaw model for neutrino masses and mixing with an $S_3 \times Z_3$ symmetry. It involves an interplay of type-I and type-II seesaw contributions of which the former is subdominant. The $S_3 \times Z_3$ quantum numbers of the fermion and scalar fields are chosen such that the type-II seesaw generates a mass matrix which incorporates the atmospheric mass splitting and sets $\theta_{23} = \pi/4$. The solar splitting and θ_{13} are absent, while the third mixing angle can achieve any value, θ_{12}^0. Specific choices of θ_{12}^0 are of interest, e.g., 35.3° (tribimaximal), 45.0° (bimaximal), 31.7° (golden ratio), and 0° (no solar mixing). The role of the type-I seesaw is to nudge all the above into the range indicated by the data. The model results in novel interrelationships between these quantities due to their common origin, making it readily falsifiable. For example, normal (inverted) ordering is associated with θ_{23} in the first (second) octant. *CP* violation is controlled by phases in the right-handed neutrino Majorana mass matrix, $M_{\nu R}$. In their absence, only normal ordering is admissible. When $M_{\nu R}$ is complex, the Dirac *CP* phase, δ, can be large, i.e., $\sim \pm \pi/2$, and inverted ordering is also allowed. The preliminary results from T2K and NOVA which favor normal ordering and $\delta \sim -\pi/2$ are indicative, in this model, of a lightest neutrino mass of 0.05 eV or more.

DOI: 10.1103/PhysRevD.94.115028

I. INTRODUCTION

Oscillation experiments over vastly different baselines and a range of neutrino energies have filled up a large portion of the mass and mixing jigsaw of the neutrino sector. Yet, we still remain in the dark with regard to *CP* violation in the lepton sector. Neither do we know the mass ordering—whether it is normal or inverted. Further open issues are the absolute mass scale of neutrinos and whether they are of Majorana or Dirac nature. While we await experimental guidance for each of the above unknowns, there have been many attempts to build models of lepton mass which capture much of what is known.

Here, we propose a neutrino mass model based on the direct product group $S_3 \times Z_3$. The elements of S_3[1] correspond to the permutations of three objects. Needless to say, S_3-based models of neutrino mass were considered earlier [1,2]. A popular point of view [3] has been to note that a permutation symmetry between the three neutrino states is consistent with[2] (a) a democratic mass matrix, $M_{\rm dem}$, all the elements of which are equal, and (b) a mass matrix proportional to the identity matrix, I. A general combination of these two forms, e.g., $c_1 I + c_2 M_{\rm dem}$, where c_1, c_2 are complex numbers, provides a natural starting point. One of the eigenstates, namely, an equal weighted combination of the three states, is one column of the popular tribimaximal mixing matrix. Many models have been presented [3] which add perturbations to this structure to accomplish realistic neutrino masses and mixing. Variations on this theme [4] explore mass matrices with such a form in the context of Grand Unified Theories, in models of extra dimensions, and examine renormalization group effects on such a pattern realized at a high energy. Other variants of the S_3-based models, for example, Ref. [5], rely on a 3-3-1 local gauge symmetry, tie it to a $(B-L)$-extended model, or realize specific forms of mass matrices through soft symmetry breaking, etc. As discussed later, the irreducible representations of S_3 are one and two dimensional. The latter provides a natural mechanism to get maximal mixing in the $\nu_\mu - \nu_\tau$ sector [6].

The present work, also based on S_3 symmetry, breaks new ground in the following directions. First, it involves an interplay of type-I and type-II seesaw contributions. Second, it presents a general framework encompassing many popular mixing patterns such as tribimaximal mixing. Further, the model does not invoke any soft symmetry-breaking terms. All the symmetries are broken spontaneously.

We briefly outline here the strategy of this work. We use the standard notation for the leptonic mixing matrix—the Pontecorvo, Maki, Nakagawa, Sakata (PMNS) matrix—U,

*soumitapramanick5@gmail.com
†palitprof@gmail.com

[1]More details of S_3 can be found in Appendix A.

[2]Note, however, there is no three-dimensional irreducible representation of S_3 (see Appendix A). So these models entail fine-tuning.

$$U = \begin{pmatrix} c_{12}c_{13} & s_{12}c_{13} & s_{13}e^{-i\delta} \\ -c_{23}s_{12} + s_{23}s_{13}c_{12}e^{i\delta} & c_{23}c_{12} + s_{23}s_{13}s_{12}e^{i\delta} & s_{23}c_{13} \\ s_{23}s_{12} + c_{23}s_{13}c_{12}e^{i\delta} & -s_{23}c_{12} + c_{23}s_{13}s_{12}e^{i\delta} & c_{23}c_{13} \end{pmatrix}, \tag{1}$$

where $c_{ij} = \cos\theta_{ij}$ and $s_{ij} = \sin\theta_{ij}$. The neutrino masses and mixings arise through a two-stage mechanism. In the first step, from the type-II seesaw, the larger atmospheric mass splitting, $\Delta m^2_{\rm atmos}$, is generated while the solar splitting, $\Delta m^2_{\rm solar}$, is absent. Also, $\theta_{13} = 0$, $\theta_{23} = \pi/4$, and the model parameters can be continuously varied to obtain any desired θ^0_{12}. Of course, in reality $\theta_{13} \neq 0$ [7], the solar splitting is nonzero, and there are indications that θ_{23} is large but nonmaximal. Experiments have also set limits on θ_{12}. The type-I seesaw addresses all the above issues and relates the masses and mixings to each other.

The starting form incorporates several well-studied mixing patterns such as tribimaximal (TBM), bimaximal (BM), and golden ratio (GR) mixings within its fold. These alternatives all have $\theta_{13} = 0$ and $\theta_{23} = \pi/4$. They differ only in the value of the third mixing angle θ^0_{12} as displayed in Table I. The fourth option in this table, no solar mixing (NSM), exhibits the attractive feature[3] that the mixing angles are either maximal, i.e., $\pi/4$ (θ_{23}), or vanishing (θ_{13} and θ^0_{12}).

In the following section, we furnish a description of the model including the assignment of $S_3 \times Z_3$ quantum numbers to the leptons and symmetry-breaking scalar fields. The consequences of the model are described next, where we also compare with the experimental data. A summary and conclusions follow. The scalar potential of this model has a rich structure. In two Appendixes, we present the essence of S_3 symmetry and discuss the S_3 invariant scalar potential, deriving the conditions which must be satisfied by the scalar coefficients to obtain the desired minimum.

II. MODEL

In the model under discussion, fermion and scalar multiplets are assigned $S_3 \times Z_3$ quantum numbers in a manner such that spontaneous symmetry breaking naturally yields mass matrices which lead to the seesaw features espoused earlier. All terms allowed by the symmetries of the model are included in the Lagrangian. No soft symmetry-breaking terms are required.

To begin, it will be useful to formulate the conceptual structure behind the model. Neutrino masses arise from a combination of type-I and type-II seesaw contributions, of which the latter dominates. In the neutrino mass basis, which is also the basis in which the Lagrangian will be presented, the type-II seesaw yields a diagonal matrix in which two states are degenerate:

$$M_{\nu L} = \begin{pmatrix} m_1^{(0)} & 0 & 0 \\ 0 & m_1^{(0)} & 0 \\ 0 & 0 & m_3^{(0)} \end{pmatrix}. \tag{2}$$

This mass matrix results in $\Delta m^2_{\rm atmos} = (m_3^{(0)})^2 - (m_1^{(0)})^2$, while $\Delta m^2_{\rm solar} = 0$. Later, we find the combinations $m^{\pm} = m_3^{(0)} \pm m_1^{(0)}$ useful. m^- signals the mass ordering; it is positive for normal ordering and negative for inverted ordering.

At this stage, the mixing resides entirely in the charged lepton sector. We follow the convention

$$\Psi_{\rm flavour} = U_\Psi \Psi_{\rm mass}, \tag{3}$$

for the fermions Ψ, so that the PMNS matrix, U, is given by

$$U = U_l^\dagger U_\nu. \tag{4}$$

TABLE I. The solar mixing angle, θ^0_{12} for this work, for the TBM, BM, and GR mixing patterns. NSM stands for the case where the solar mixing angle is initially vanishing.

Model	TBM	BM	GR	NSM
θ^0_{12}	35.3°	45.0°	31.7°	0.0°

TABLE II. The fermion content of the model. The transformation properties under S_3, Z_3, and $SU(2)_L$ are shown. The hypercharge of the fields, Y, and their lepton number, L, are also indicated. Here, $L^T_\alpha = (\nu_\alpha\ l^-_\alpha)$.

Fields	Notations	S_3 (Z_3)	$SU(2)_L(Y)$	L
Left-handed leptons	L_e	$1'(1)$		
	L_μ	$1'(\omega)$	2 (−1)	+1
	L_τ	1 (ω)		
Right-handed	e_R	$1'(1)$		
charged leptons	$\begin{pmatrix}\mu_R \\ \tau_R\end{pmatrix}$	2(1)	1 (−2)	+1
Right-handed neutrinos	N_{1R}	$1'(1)$		
	N_{2R}	$1'(\omega)$	1 (0)	0
	N_{3R}	1 (ω)		

[3]Such a mixing pattern was envisioned earlier in a model based on $A4$ symmetry [8] which built on previous work along similar lines [9,10].

TABLE III. The scalar content of the model. The transformation properties under S_3, Z_3, and $SU(2)_L$ are shown. The hypercharge of the fields, Y; their lepton number, L; and the vacuum expectation values are also indicated. $w_i (i = 1…4)$ are dimensionless.

Purpose	Notations	S_3 (Z_3)	$SU(2)_L$ (Y)	L	vev
Charged fermion mass	$\eta \equiv (\eta^+ \eta^0)$	1 (1)	2 (1)	0	$\langle\eta\rangle = v_\eta(0\ 1)$
	$\Phi_a \equiv \begin{pmatrix} \phi_1^+ & \phi_1^0 \\ \phi_2^+ & \phi_2^0 \end{pmatrix}$	2 (1)	2 (1)	0	$\langle\Phi_a\rangle = \frac{v_a}{\sqrt{2}}\begin{pmatrix} 0 & w_1 \\ 0 & w_2 \end{pmatrix}$
	$\Phi_b \equiv \begin{pmatrix} \phi_3^+ & \phi_3^0 \\ \phi_4^+ & \phi_4^0 \end{pmatrix}$	2 (ω)	2 (1)	0	$\langle\Phi_b\rangle = \frac{v_b}{\sqrt{2}}\begin{pmatrix} 0 & w_3 \\ 0 & w_4 \end{pmatrix}$
	$\alpha \equiv (\alpha^+ \ \alpha^0)$	1 (ω)	2 (1)	0	$\langle\alpha\rangle = v_\alpha(0\ 1)$
Neutrino Dirac mass	$\beta \equiv (\beta^0 \ \beta^-)$	1 (1)	2 (-1)	1	$\langle\beta\rangle = v_\beta(1\ 0)$
Type-II seesaw mass	$\Delta_L \equiv (\Delta_L^{++}, \Delta_L^+, \Delta_L^0)$	1 (1)	3 (2)	−2	$\langle\Delta_L\rangle = v_\Delta(0\ 0\ 1)$
	$\rho_L \equiv (\rho_L^{++}, \rho_L^+, \rho_L^0)$	1 (ω)	3 (2)	−2	$\langle\rho_L\rangle = v_\rho(0\ 0\ 1)$
Right-handed neutrino mass	$\chi \equiv \chi^0$	1 (ω)	1 (0)	0	$\langle\chi\rangle = u_\chi$
	$\gamma \equiv \gamma^0$	1′(ω)	1 (0)	0	$\langle\gamma\rangle = u_\gamma$

As noted, at this level $\theta_{12} = \theta_{12}^0$, where alternate choices of θ_{12}^0 result in popular mixing patterns such as tribimaximal, bimaximal, and golden ratio with the common feature that $\theta_{13} = 0$ and $\theta_{23} = \pi/4$. $\theta_{12}^0 = 0$ is another interesting alternative [8] where initially the lepton mixing angles are either vanishing $\theta_{13} = 0 = \theta_{12}$ or maximal, i.e., $\pi/4$ (θ_{23}). Thus, until type-I seesaw effects are included, the leptonic mixing matrix takes the form

$$U^0 = \begin{pmatrix} \cos\theta_{12}^0 & \sin\theta_{12}^0 & 0 \\ -\frac{\sin\theta_{12}^0}{\sqrt{2}} & \frac{\cos\theta_{12}^0}{\sqrt{2}} & \frac{1}{\sqrt{2}} \\ \frac{\sin\theta_{12}^0}{\sqrt{2}} & -\frac{\cos\theta_{12}^0}{\sqrt{2}} & \frac{1}{\sqrt{2}} \end{pmatrix} = U_l^\dagger U_\nu^0, \qquad (5)$$

where $U_\nu^0 = I$ and the charged lepton mass matrix is

$$M_{e\mu\tau} = U_l \begin{pmatrix} m_e & 0 & 0 \\ 0 & m_\mu & 0 \\ 0 & 0 & m_\tau \end{pmatrix} I = \begin{pmatrix} m_e\cos\theta_{12}^0 & -\frac{m_\mu}{\sqrt{2}}\sin\theta_{12}^0 & \frac{m_\tau}{\sqrt{2}}\sin\theta_{12}^0 \\ m_e\sin\theta_{12}^0 & \frac{m_\mu}{\sqrt{2}}\cos\theta_{12}^0 & -\frac{m_\tau}{\sqrt{2}}\cos\theta_{12}^0 \\ 0 & \frac{m_\mu}{\sqrt{2}} & \frac{m_\tau}{\sqrt{2}} \end{pmatrix}. \qquad (6)$$

The identity matrix, I, at the right in the first step above indicates that no transformation needs to be applied on the right-handed charged leptons which are $SU(2)_L$ singlets.

In this basis, the matrices responsible for the type-I seesaw have the forms

$M_D = m_D \mathbb{I}$ and

$$M_{\nu R} = \frac{m_R}{2xy}\begin{pmatrix} 0 & xe^{-i\phi_1} & xe^{-i\phi_1} \\ xe^{-i\phi_1} & ye^{-i\phi_2}/\sqrt{2} & -ye^{-i\phi_2}/\sqrt{2} \\ xe^{-i\phi_1} & -ye^{-i\phi_2}/\sqrt{2} & ye^{-i\phi_2}/\sqrt{2} \end{pmatrix}, \qquad (7)$$

where m_D and m_R set the scale for the Dirac and right-handed Majorana masses while x and y are dimensionless real quantities of $\mathcal{O}(1)$. We take the Dirac mass matrix M_D proportional to the identity for ease of presentation. We have checked that the same results can be reproduced so long as M_D is diagonal. The right-handed neutrino Majorana mass matrix, $M_{\nu R}$, has a $N_{2R} \leftrightarrow N_{3R}$ discrete symmetry. This choice, too, can be relaxed without jeopardizing the final outcome.

We will show later how the mass matrices in Eqs. (2)–(7) lead to a good fit to the neutrino data and yield testable predictions. But before this, we must ensure that the above matrices can arise from the $S_3 \times Z_3$ symmetric Lagrangian.

The behavior of the fermions, i.e., the three lepton generations[4] including three right-handed neutrinos, is summarized in Table II. The gauge interactions of the leptons are universal and diagonal in this basis. A feature worth noting is that the right-handed neutrinos have lepton number $L = 0$. We discuss later how this leads to a diagonal neutrino Dirac mass matrix. The lepton mass matrices arise from the Yukawa couplings allowed by the $S_3 \times Z_3$ symmetry.

The $S_3 \times Z_3$ structure of the lepton sector is matched by a rich scalar sector which we have presented in Table III. The requirement of charged lepton masses and type-I and type-II seesaw neutrino masses dictates the inclusion of $SU(2)_L$ singlet, doublet, and triplet scalar fields. The $S_3 \times Z_3$ properties of the scalars are chosen bearing in mind the S_3 and Z_3 combination rules. In particular, for the former,

[4]The scope of this model is restricted to the lepton sector.

the representations are 1, 1′, and 2 which satisfy the multiplication rules (see Appendix A):

$$1 \times 1' = 1', \qquad 1' \times 1' = 1, \quad \text{and} \quad 2 \times 2 = 2 + 1 + 1'. \tag{8}$$

The scalar multiplets are chosen such that the mass matrices appear with specific structures as discussed below.[5] It can be seen from Table III that all neutral scalars pick up a vacuum expectation value (vev). The vev of the $SU(2)_L$ singlets, namely, u_χ and u_γ, can be much higher than the electroweak scale, v, and determine the masses of the right-handed neutrinos. The other vev break $SU(2)_L$. We take $v_\Delta \sim v_\rho \ll v_\eta \sim v_a \sim v_b \sim v_\alpha \sim v_\beta \sim v$.

Charged lepton and neutrino masses are obtained from the Yukawa terms in a Lagrangian constructed out of the fields in Tables II and III. Including all terms which respect the $SU(2)_L \times U(1)_Y$ gauge symmetry and the $S_3 \times Z_3$ flavor symmetry so long as lepton number, L, is also conserved, one is led to the Lagrangian mass terms

$$\begin{aligned}
\mathcal{L}_{\text{mass}} &= f_1 \bar{e}_L(\mu_R \phi_2^0 - \tau_R \phi_1^0) + f_2 \bar{\mu}_L(\mu_R \phi_4^0 - \tau_R \phi_3^0) + f_3 \bar{\tau}_L(\mu_R \phi_4^0 + \tau_R \phi_3^0) \\
&+ f_4 \bar{\mu}_L e_R \alpha^0 + f_5 \bar{e}_L e_R \eta^0 \quad \text{(charged lepton mass)} \\
&+ (h_1 \bar{\nu}_{eL} N_{1R} + h_2 \bar{\nu}_{\mu L} N_{2R} + h_3 \bar{\nu}_{\tau L} N_{3R}) \beta^0 \quad \text{(neutrino Dirac mass)} \\
&+ \frac{1}{2} g_1 \nu_{eL}^T C^{-1} \nu_{eL} \Delta_L^0 + \frac{1}{2}(g_2 \nu_{\mu L}^T C^{-1} \nu_{\mu L} + g_3 \nu_{\tau L}^T C^{-1} \nu_{\tau L}) \rho_L \quad \text{(neutrino type-II seesaw mass)} \\
&+ \frac{1}{2}([k_1 N_{2R}^T C^{-1} N_{2R} + k_2 N_{3R}^T C^{-1} N_{3R}]\chi + k_3 N_{2R}^T C^{-1} N_{3R} \gamma) \\
&+ \frac{1}{2}(k_4 N_{1R}^T C^{-1} N_{2R} \tilde{\chi} + k_5 N_{1R}^T C^{-1} N_{3R} \tilde{\gamma}) \quad \text{(rh neutrino mass)} + \text{h.c.}.
\end{aligned} \tag{9}$$

Here, $\tilde{\chi}$ and $\tilde{\gamma}$ are charge conjugated fields which transform under Z_3 as ω^2. For each term in the Lagrangian, the fermion masses which arise therefrom have been indicated. Both type-I and type-II seesaw contributions for neutrino masses are present.

The above Lagrangian gives rise to the mass matrices in Eqs. (2)–(7) through the Yukawa couplings in Eq. (9) and the vevs in Table III. Before turning to these, let us note how the quantum number assignments of the fermion and scalar fields force certain entries in the mass matrices to be vanishing. For example, the mass term $\bar{\tau}_L e_R$ is zero in Eq. (6) because there is no $SU(2)_L$ doublet field which transforms as a $1'$ under S_3. Similarly, the diagonal nature of the left-handed neutrino Majorana mass matrix in Eq. (2) is ensured by the absence of an $SU(2)_L$ triplet field which transforms either as (i) a $1'$ under S_3 or (ii) as ω^2 under Z_3. The neutrino Dirac mass matrix in Eq. (7) arises from the Yukawa couplings[6] of the $SU(2)_L$ doublet scalar β. Since it transforms as 1 under both S_3 and Z_3, it can be seen from the left-handed and right-handed neutrino quantum numbers in Table II that only diagonal terms are allowed. Finally, the $N_{1R}^T N_{1R}$ term is absent in the right-handed neutrino Majorana mass matrix in Eq. (7) since there is no Z_3 singlet among the $SU(2)_L$ singlet scalars.

[5]In general, the multiple scalar fields in models based on discrete symmetries also result in flavor changing neutral currents induced by the neutral scalars. Discussions of this aspect in the context of S_3 can be found, for example, in Ref. [11].

[6]As the N_{iR} carry $L = 0$, conservation of the lepton number forbids any contribution to the Dirac mass from the $SU(2)_L$ scalar doublets which generate the charged lepton masses.

Before proceeding further, it may be useful to comment on the sizes of the various vacuum expectation values in Table III. The $SU(2)_L$ doublets acquire vevs $v_{\eta,a,b,\alpha,\beta}$ which are $\mathcal{O}(M_W)$, while the triplet vevs $v_{\Delta,\rho}$ are several orders of magnitude smaller. This is in consonance with the smallness of the neutrino masses and also the ρ parameter of electroweak symmetry breaking. Needless to say, the $SU(2)_L$ singlet fields χ and γ can acquire vevs well above the electroweak scale.

The nonvanishing entries in the mass matrices in Eqs. (2)–(7) which arise from the Yukawa couplings entail the following relationships:

(1) Charged lepton masses—On matching the Lagrangian in Eq. (9), the scalar doublet vevs in Table III, and the charged lepton mass matrix in Eq. (6), one gets

$$f_1\langle\phi_1^0\rangle = -\frac{m_\tau}{\sqrt{2}}\sin\theta_{12}^0, \qquad f_1\langle\phi_2^0\rangle = -\frac{m_\mu}{\sqrt{2}}\sin\theta_{12}^0, \tag{10}$$

$$f_2\langle\phi_3^0\rangle = \frac{m_\tau}{\sqrt{2}}\cos\theta_{12}^0, \qquad f_2\langle\phi_4^0\rangle = \frac{m_\mu}{\sqrt{2}}\cos\theta_{12}^0,$$

$$f_3\langle\phi_3^0\rangle = \frac{m_\tau}{\sqrt{2}}, \qquad f_3\langle\phi_4^0\rangle = \frac{m_\mu}{\sqrt{2}}, \tag{11}$$

and

$$f_4\langle\alpha^0\rangle = m_e \sin\theta_{12}^0, \qquad f_5\langle\eta^0\rangle = m_e \cos\theta_{12}^0. \tag{12}$$

Notice that Eqs. (10) and (11) imply

$$\frac{w_2}{w_1} = \frac{w_4}{w_3} = \frac{m_\mu}{m_\tau}. \tag{13}$$

(2) Left-handed neutrino Majorana mass—Similarly, the mass matrix in Eq. (2) is obtained when

$$g_1\langle\Delta_L^0\rangle = m_1^0 = g_2\langle\rho_L^0\rangle, \qquad g_3\langle\rho_L^0\rangle = m_3^0. \tag{14}$$

The first equation above requires a matching between two sets of Yukawa couplings and vevs. This is to ensure the degeneracy of two neutrino states, implying the vanishing of the solar mass splitting at this stage. Notice that the relatively large size of the atmospheric mass splitting requires g_2 and g_3 to be of different order.

(3) Neutrino Dirac mass—The Dirac mass matrix in Eq. (7) is due to the relations

$$h_1 = h_2 = h_3 = h \quad \text{and} \quad h\langle\beta^0\rangle = m_D. \tag{15}$$

The equality of the three Yukawa couplings, h_i, above is only a simplified choice. We have checked that deviations from this relation, i.e., a diagonal Dirac mass matrix but not proportional to the identity, can also readily lead to the results which we discuss in this paper.

(4) Right-handed neutrino Majorana mass—Finally, the right-handed neutrino Majorana mass matrix follows from

$$\begin{aligned} k_1\langle\chi^0\rangle &= \frac{m_R e^{-i\phi_2}}{2\sqrt{2}x} = k_2\langle\chi^0\rangle, \\ k_3\langle\gamma^0\rangle &= -\frac{m_R e^{-i\phi_2}}{2\sqrt{2}x}, \\ k_4\langle\tilde{\chi}^0\rangle &= \frac{m_R e^{-i\phi_1}}{2y} = k_5\langle\tilde{\gamma}^0\rangle. \end{aligned} \tag{16}$$

We show in Appendix B how from a minimization of the scalar potential the required scalar vevs may be obtained.

A. Type-I seesaw contribution

In the previous section, we have shown that the S_3 model results in a diagonal left-handed neutrino mass matrix given in Eq. (2) through a type-II seesaw. The charged lepton mass matrix as given in Eq. (6) is not diagonal and induces a mixing in the lepton sector. This mixing, Eq. (5), receives further corrections from a smaller type-I seesaw contribution to the neutrino mass matrix as we discuss.

The type-I seesaw arising from the Dirac and right-handed neutrino mass matrices in Eq. (7) is

$$M' = [M_D^T(M_{\nu R})^{-1}M_D] = \frac{m_D^2}{m_R}\begin{pmatrix} 0 & ye^{i\phi_1} & ye^{i\phi_1} \\ ye^{i\phi_1} & \frac{xe^{i\phi_2}}{\sqrt{2}} & \frac{-xe^{i\phi_2}}{\sqrt{2}} \\ ye^{i\phi_1} & \frac{-xe^{i\phi_2}}{\sqrt{2}} & \frac{xe^{i\phi_2}}{\sqrt{2}} \end{pmatrix}. \tag{17}$$

III. RESULTS

We have given above the contributions to the neutrino mass matrix from the type-I and type-II seesaw. Of these, the former is taken to be significantly smaller than the latter. As we have noted, in the absence of the type-I seesaw, the leptonic mixing matrix in this model is determined entirely by the charged lepton mass matrix. It has $\theta_{13} = 0$, $\theta_{23} = \pi/4$, and θ_{12} arbitrary. We will be considering four mixing patterns which fall within this scheme and in each of which the value of θ_{12}^0 is specified, namely, the TBM, BM, GR, and NSM cases. In addition, in this model, the type-II seesaw sets the solar mass splitting to be zero. The type-I seesaw, the effect of which we incorporate perturbatively, brings all the above leptonic parameters into agreement with their values preferred by the data. Before we proceed further with this discussion, it will be useful to summarize the global best-fit values of these mass splittings and angles.

A. Data

From global fits, the currently favored 3σ ranges of the neutrino mixing parameters are [12,13]

$$\begin{aligned} &\Delta m_{21}^2 = (7.02\text{–}8.08)\times 10^{-5}\ \text{eV}^2, \quad \theta_{12} = (31.52\text{–}36.18)^\circ, \\ &|\Delta m_{31}^2| = (2.351\text{–}2.618)\times 10^{-3}\ \text{eV}^2, \quad \theta_{23} = (38.6\text{–}53.1)^\circ, \\ &\theta_{13} = (7.86\text{–}9.11)^\circ, \quad \delta = (0-360)^\circ. \end{aligned} \tag{18}$$

These data are from NuFIT2.1 of 2016 [12]. Here, $\Delta m_{ij}^2 = m_i^2 - m_j^2$, so that $\Delta m_{31}^2 > 0 (< 0)$ for normal (inverted) ordering. The data indicate two best-fit points for θ_{23} in the first and second octants. Later, we also remark about the compatibility of this model with the recent T2K and NOVA hints [14,15] of δ being near $-\pi/2$.

B. Real $M_{\nu R}$ ($\phi_1 = 0$ or π, $\phi_2 = 0$, or π)

A limiting case, with less complications, corresponds to no CP violation. This happens when $M_{\nu R}$ is real, i.e., the phases $\phi_{1,2}$ in Eq. (17) are 0 or π. These cases can be compactly considered by keeping x and y real but allowing them to be of either sign, i.e., four alternatives. We show below how the experimental data pick out one or the other out of these.

Without the phases $\phi_{1,2}$, i.e., for real $M_{\nu R}$, one gets

$$M' = \frac{m_D^2}{m_R}\begin{pmatrix} 0 & y & y \\ y & \frac{x}{\sqrt{2}} & -\frac{x}{\sqrt{2}} \\ y & -\frac{x}{\sqrt{2}} & \frac{x}{\sqrt{2}} \end{pmatrix}. \tag{19}$$

The equality of two neutrino masses from the type-II seesaw requires the use of degenerate perturbation theory to obtain corrections to the solar mixing parameters. The 2×2 submatrix of M' relevant for this is

TABLE IV. The ranges of ζ [Eq. (21)], ϵ [Eq. (22)], and $(\epsilon - \theta_{12}^0)$ allowed by the data for the different popular mixing patterns.

Model (θ_{12}^0)	TBM (35.3°)	BM (45.0°)	GR (31.7°)	NSM (0.0°)
ζ	$-4.0° \leftrightarrow 0.6°$	$-13.7° \leftrightarrow -9.1°$	$-0.4° \leftrightarrow 4.2°$	$31.3° \leftrightarrow 35.9°$
ϵ	$-4.0° \leftrightarrow 0.6°$	$-14.5° \leftrightarrow -9.3°$	$-0.4° \leftrightarrow 4.2°$	$44.0° \leftrightarrow 56.7°$
$\epsilon - \theta_{12}^0$	$-39.2° \leftrightarrow -34.6°$	$-59.5° \leftrightarrow -54.4°$	$-39.2° \leftrightarrow -30.0°$	$44.0° \leftrightarrow 56.7°$

$$M'_{2\times 2} = \frac{m_D^2}{m_R}\begin{pmatrix} 0 & y \\ y & x/\sqrt{2} \end{pmatrix}. \tag{20}$$

This results in

$$\theta_{12} = \theta_{12}^0 + \zeta, \qquad \tan 2\zeta = 2\sqrt{2}\left(\frac{y}{x}\right). \tag{21}$$

A related quantity, ϵ, which is found useful later, is given by

$$\sin\epsilon = \frac{y}{\sqrt{y^2 + x^2/2}} \quad \text{and} \quad \cos\epsilon = \frac{x/\sqrt{2}}{\sqrt{y^2 + x^2/2}},$$
$$\text{i.e.,} \quad \tan\epsilon = \frac{1}{2}\tan 2\zeta. \tag{22}$$

Once a mixing pattern is chosen, i.e., θ_{12}^0 fixed, the experimental limits on θ_{12} as given in Eq. (18) set bounds on the range of ζ and also from Eq. (22) on ϵ. These are displayed for the four mixing patterns in Table IV. If ζ is positive (negative), then the ratio (y/x) will also be positive (negative). In addition, from Eq. (22), the sign of y is fixed by the value of ϵ. Taking these points into account, one can conclude that x is always positive, i.e., ϕ_2 has to be zero, while y must be positive, $\phi_1 = 0$ (negative, $\phi_1 = \pi$) for NSM (BM). For the other mixing patterns, i.e., TBM and GR, both signs of y are possible.

The solar mass splitting arising from the type-I seesaw is also obtained from Eq. (20).

$$\Delta m^2_{\text{solar}} = \frac{\sqrt{2}m_D^2}{m_R} m_1^{(0)} \sqrt{x^2 + 8y^2} = \frac{\sqrt{2}m_D^2}{m_R} m_1^{(0)} \frac{x}{\cos 2\zeta}. \tag{23}$$

Furthermore, incorporating the leading order corrections to neutrino mixing from Eq. (19), one gets from Eq. (4),

$$U = U^0 U_\nu \quad \text{with}$$
$$U_\nu = \begin{pmatrix} \cos\zeta & -\sin\zeta & \kappa_r \sin\epsilon \\ \sin\zeta & \cos\zeta & -\kappa_r\cos\epsilon \\ \kappa_r\sin(\zeta-\epsilon) & \kappa_r\cos(\zeta-\epsilon) & 1 \end{pmatrix}, \tag{24}$$

with

$$\kappa_r \equiv \frac{m_D^2}{m_R m^-}\sqrt{y^2 + x^2/2} = \frac{m_D^2}{m_R m^-}\frac{x}{\sqrt{2}\cos\epsilon}. \tag{25}$$

The third column of the leptonic mixing matrix becomes

$$|\psi_3\rangle = \begin{pmatrix} \kappa_r \sin(\epsilon - \theta_{12}^0) \\ \frac{1}{\sqrt{2}}[1 - \kappa_r\cos(\epsilon - \theta_{12}^0)] \\ \frac{1}{\sqrt{2}}[1 + \kappa_r\cos(\epsilon - \theta_{12}^0)] \end{pmatrix}. \tag{26}$$

Since, as noted, x is always positive, κ_r is positive (negative) for normal (inverted) ordering.

The right-hand side of Eq. (26) has to be matched with the third column of Eq. (1). This yields

$$\sin\theta_{13}\cos\delta = \kappa_r \sin(\epsilon - \theta_{12}^0), \tag{27}$$

and

$$\tan(\pi/4 - \theta_{23}) \equiv \tan\omega = \kappa_r\cos(\epsilon - \theta_{12}^0). \tag{28}$$

For ready reference, the ranges of $(\epsilon - \theta_{12}^0)$ allowed for the different mixing patterns are presented in Table IV. For normal ordering,[7] the CP phase δ is zero (π) when $\sin(\epsilon - \theta_{12}^0)$ is positive (negative). From Table IV, one can then observe that $\delta = 0$ for the NSM mixing pattern and is π for the three other cases. Needless to say, both correspond to CP conservation.

Combining Eqs. (23), (25), and (27), one can write

$$\Delta m^2_{\text{solar}} = 2m^- m_1^{(0)} \frac{\sin\theta_{13}\cos\delta\cos\epsilon}{\cos 2\zeta \sin(\epsilon - \theta_{12}^0)}. \tag{29}$$

Equation (29) leads to the conclusion that inverted ordering is not allowed for this case of real $M_{\nu R}$. To establish this property, one can define

$$z \equiv m^- m_1^{(0)}/\Delta m^2_{\text{atmos}} \quad \text{and} \quad \tan\xi \equiv m_0/\sqrt{|\Delta m^2_{\text{atmos}}|}, \tag{30}$$

where z is positive for both mass orderings. From Eq. (29), one has

$$z = \left(\frac{\Delta m^2_{\text{solar}}}{|\Delta m^2_{\text{atmos}}|}\right)\left(\frac{\cos 2\zeta \sin(\epsilon - \theta_{12}^0)}{2\sin\theta_{13}|\cos\delta|\cos\epsilon}\right). \tag{31}$$

It is easy to verify from Eq. (30) that

[7]We show in the following that inverted ordering is not consistent with real $M_{\nu R}$.

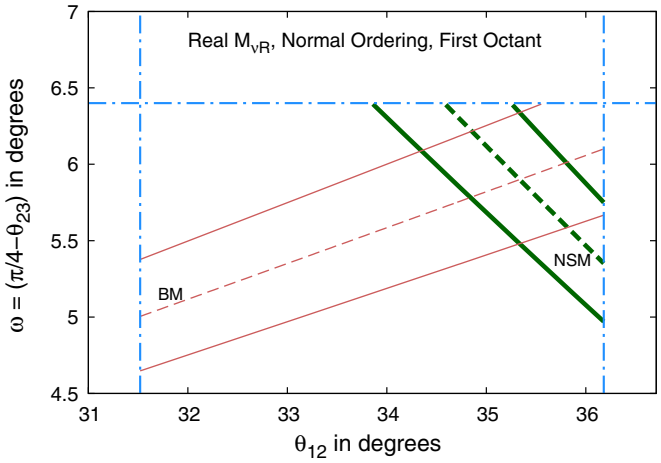

FIG. 1. $\omega = (\pi/4 - \theta_{23})$ as a function of θ_{12} for normal ordering. The solid lines indicate the range for the 3σ allowed variation of $\sin\theta_{13}$, while the dashed line corresponds to the best-fit value. Thick green (thin pink) lines are for the NSM (BM) case. The horizontal and vertical blue dot-dashed lines delimit the 3σ allowed range from data. Note that ω is always positive; i.e., the first octant of θ_{23} is preferred. For the TBM and GR mixing patterns, ω, still positive, lies beyond the 3σ range. Best-fit values of the solar and atmospheric splittings are used. For $M_{\nu R}$ real, there is no allowed solution for inverted ordering.

$$z = \sin\xi/(1+\sin\xi) \quad \text{i.e., } 0 \le z \le \frac{1}{2} \quad \text{(for normal ordering)},$$
$$z = 1/(1+\sin\xi) \quad \text{i.e., } \frac{1}{2} \le z \le 1 \quad \text{(for inverted ordering)}. \tag{32}$$

There is a one-to-one correspondence of z with the lightest neutrino mass m_0. The quasidegeneracy limit, i.e., $m_0 \to$ large, is approached as $z \to \frac{1}{2}$ for both mass orderings.

In Eq. (31), $|\cos\delta| = 1$ for real $M_{\nu R}$. Using the global fit mass splittings and mixing angles given in Sec. III A and Table IV, one finds $z \sim 10^{-2}$ or smaller for all four mixing patterns. This excludes the inverted mass ordering option for real $M_{\nu R}$.

From Eqs. (27) and (28), one has

$$\tan\omega = \frac{\sin\theta_{13}\cos\delta}{\tan(\epsilon - \theta_{12}^0)}. \tag{33}$$

The noteworthy point is that for normal ordering Eq. (28) implies that ω is always positive irrespective of the mixing pattern. So, in this model, θ_{23} is restricted to the first octant only for real $M_{\nu R}$.

Equations (21) and (22) can be used to express ϵ in terms of θ_{12} and thereby put ω in Eq. (33) as a function of θ_{12} and θ_{13} only. In Fig. 1, ω is shown as a function of θ_{12} for the NSM (thick green lines) and BM (thin pink lines) mixing patterns. The ranges of θ_{12} and ω have been kept within their 3σ allowed limits from global fits as given in Sec. III A. The TBM and GR cases are excluded because for the allowed values of θ_{12} they predict θ_{23} beyond the 3σ range. The solid lines in the figure correspond to the 3σ limiting values of θ_{13}, and the dashed line is for its best-fit value. The blue dot-dashed horizontal and vertical lines display the 3σ experimental bounds on θ_{23} and θ_{12}.

Using Eq. (31), any allowed point in the $\omega - \theta_{12}$ plane and the associated θ_{13} can be translated to a value of z or equivalently m_0, provided the solar and atmospheric mass splittings are given. We find that for both the allowed mixing patterns the range of variation of m_0 is very small. For the NSM (BM) case, this range is 2.13 meV $\le m_0 \le$ 3.10 meV (3.20 meV $\le m_0 \le$ 4.42 meV) when both neutrino mass splittings and all mixing angles are varied over their full 3σ ranges.

To summarize the real $M_{\nu R}$ case:

(1) Only the normal mass ordering is allowed.
(2) θ_{23} can lie only in the first octant.
(3) The TBM and GR alternatives are inconsistent with the allowed ranges of the neutrino mixing angles even after including the type-I seesaw corrections.
(4) For the NSM and BM mixing patterns, real $M_{\nu R}$ can give consistent solutions for the neutrino masses and mixings. The ranges of allowed lightest neutrino masses are very tiny.

C. Complex $M_{\nu R}$

Keeping $M_{\nu R}$ real eliminates CP violation. Further, inverted ordering is disallowed. Also, the TBM and GR mixing patterns cannot be accommodated. These restrictions can be ameliorated by taking $M_{\nu R}$ in its general complex form giving rise to the type-I seesaw contribution M' as given in Eq. (17). Recall that this introduces the phases $\phi_{1,2}$ and x, y take only positive values.

With its complex entries, M' is now not Hermitian any more. To address this, we consider the combination $(M^0+M')^\dagger(M^0+M')$ and treat $M^{0\dagger}M^0$ as the leading term with $(M^{0\dagger}M' + M'^\dagger M^0)$ acting as a perturbation at the lowest order, both Hermitian by construction. The unperturbed eigenvalues are thus $(m_i^{(0)})^2$. The perturbation matrix is

$$(M^{0\dagger}M' + M'^\dagger M^0) = \frac{m_D^2}{m_R}\begin{pmatrix} 0 & 2ym_1^{(0)}\cos\phi_1 & yf(\phi_1) \\ 2ym_1^{(0)}\cos\phi_1 & \sqrt{2}xm_1^{(0)}\cos\phi_2 & -\frac{x}{\sqrt{2}}f(\phi_2) \\ yf^*(\phi_1) & -\frac{x}{\sqrt{2}}f^*(\phi_2) & \sqrt{2}xm_3^{(0)}\cos\phi_2 \end{pmatrix}. \tag{34}$$

In the above,

$$f(\varphi) = m^+\cos\varphi - im^-\sin\varphi. \tag{35}$$

TABLE V. Quadrants of the leptonic CP phase δ and the octant of θ_{23} for both mass orderings for different mixing patterns.

	Normal ordering		Inverted ordering	
Mixing pattern	δ quadrant	θ_{23} octant	δ quadrant	θ_{23} octant
NSM	First/fourth	First	Second/third	Second
BM, TBM, GR	Second/third	First	First/fourth	Second

The remaining calculation proceeds in much the same manner as for real $M_{\nu R}$ while keeping the distinctive features of Eq. (34) in mind.

In place of Eqs. (21) and (22) for the real $M_{\nu R}$ case, we get from (34)

$$\theta_{12} = \theta_{12}^0 + \zeta, \qquad \tan 2\zeta = 2\sqrt{2}\frac{y\cos\phi_1}{x\cos\phi_2}, \tag{36}$$

and

$$\sin\epsilon = \frac{y\cos\phi_1}{\sqrt{y^2\cos^2\phi_1 + x^2\cos^2\phi_2/2}},$$
$$\cos\epsilon = \frac{x\cos\phi_2/\sqrt{2}}{\sqrt{y^2\cos^2\phi_1 + x^2\cos^2\phi_2/2}}, \qquad \tan\epsilon = \frac{1}{2}\tan 2\zeta. \tag{37}$$

The allowed ranges of ζ and ϵ depend on the mixing pattern and are given in Table IV. It is seen that for all patterns $\cos\epsilon$ is positive. Therefore, from Eq. (37), we can immediately conclude that ϕ_2 must be always in the first or fourth quadrant. The possible quadrants of ϕ_1 are also determined from the range of ϵ for the different mixing patterns. From the first relation in Eq. (37), we find that ϕ_1 has to be in the first or fourth (second or third) quadrant if ϵ is positive (negative). Using the results in Table IV, we conclude that the first (second) option is valid for the NSM (BM) patterns. For the TBM and GR cases, ϵ spans a range over positive and negative values, and so both options are included.

The solar mass splitting is induced entirely through the type-I seesaw contribution. From Eq. (34), one finds

$$\Delta m^2_{\rm solar} = \sqrt{2}m_1^{(0)}\frac{m_D^2}{m_R}\sqrt{x^2\cos^2\phi_2 + 8y^2\cos^2\phi_1}$$
$$= \sqrt{2}m_1^{(0)}\frac{m_D^2}{m_R}\frac{x\cos\phi_2}{\cos 2\zeta} = \sqrt{2}m_1^{(0)}\frac{m_D^2}{m_R}\frac{2\sqrt{2}y\cos\phi_1}{\sin 2\zeta}. \tag{38}$$

Equation (26) is now replaced by

$$|\psi_3\rangle = \begin{pmatrix} \kappa_c[\frac{\sin\epsilon}{\cos\phi_1}f(\phi_1)\cos\theta_{12}^0 - \frac{\cos\epsilon}{\cos\phi_2}f(\phi_2)\sin\theta_{12}^0]/m^+ \\ \frac{1}{\sqrt{2}}\{1 - \kappa_c[\frac{\sin\epsilon}{\cos\phi_1}f(\phi_1)\sin\theta_{12}^0 + \frac{\cos\epsilon}{\cos\phi_2}f(\phi_2)\cos\theta_{12}^0]/m^+\} \\ \frac{1}{\sqrt{2}}\{1 + \kappa_c[\frac{\sin\epsilon}{\cos\phi_1}f(\phi_1)\sin\theta_{12}^0 + \frac{\cos\epsilon}{\cos\phi_2}f(\phi_2)\cos\theta_{12}^0]/m^+\} \end{pmatrix}, \tag{39}$$

where

$$\kappa_c = \frac{m_D^2}{m_R m^-}\sqrt{y^2\cos^2\phi_1 + x^2\cos^2\phi_2/2}, \tag{40}$$

Eq. (37) has been used, and the complex function $f(\phi_{1,2})$ is defined in Eq. (35).

κ_c is positive (negative) for normal (inverted) ordering. Comparing the right-hand side of Eq. (39) with the third column of Eq. (1), we find

$$\sin\theta_{13}\cos\delta = \kappa_c\sin(\epsilon - \theta_{12}^0), \tag{41}$$

$$\sin\theta_{13}\sin\delta = \kappa_c\frac{m^-}{m^+\cos\phi_1\cos\phi_2} \times [\sin\epsilon\sin\phi_1\cos\phi_2\cos\theta_{12}^0 - \cos\epsilon\cos\phi_1\sin\phi_2\sin\theta_{12}^0]. \tag{42}$$

As indicated in Table IV, $(\epsilon - \theta_{12}^0)$ always remains in the first (fourth) quadrant for the NSM (BM, TBM, and GR) mixing pattern. For normal ordering, Eq. (41) then implies that for the NSM (BM, TBM, and GR) case(s) δ lies in the first or fourth (second or third) quadrant. For inverted ordering of masses, κ_c changes sign, and so the quadrants are accordingly modified. The different possibilities are indicated in Table V. For any mixing pattern and mass ordering, there are two allowed quadrants of δ which have $\sin\delta$ of opposite sign. Which of these is chosen is determined by the phases $\phi_{1,2}$ through the sign of the right-hand side of Eq. (42). As noted above, ϕ_2 can be in either the first or fourth quadrants, and the quadrant of ϕ_1 is determined by the mixing pattern in such a way that $\sin\phi_1$ can be of either sign. Thus, the phases ϕ_1 and ϕ_2 can always be chosen such that $\sin\delta$ can be of any particular sign. Therefore, the two alternate quadrants of δ for every case in Table V are equally viable in this model.

TABLE VI. The group table for S_3.

	I	A	B	C	D	F
I	I	A	B	C	D	F
A	A	I	C	B	F	D
F	F	C	I	D	A	B
C	C	F	D	I	B	A
D	D	B	A	F	I	C
B	B	D	F	A	C	I

The perturbative type-I seesaw contribution to θ_{23} can also be extracted from Eq. (39). One finds

$$\tan\omega = \frac{\sin\theta_{13}\cos\delta}{\tan(\epsilon-\theta_{12}^0)}. \tag{43}$$

Recalling that Eq. (41) correlates δ and $(\epsilon-\theta_{12}^0)$ through κ_c, one can readily conclude that for all mixing patterns θ_{23} always lies in the first (second) octant for normal (inverted) ordering. This important conclusion from these models is shown in Table V.

In the expression for the solar mass splitting in Eq. (38), one can trade the factor m_D^2/m_R in terms of κ_c and use Eq. (41) to get

$$\Delta m^2_{\rm solar} = \frac{2m^- m_1^{(0)}\sin\theta_{13}\cos\delta\cos\epsilon}{\sin(\epsilon-\theta_{12}^0)cos2\zeta}. \tag{44}$$

The strategy that we have followed to extract the predictions of this model relies on utilizing Eqs. (43) and (44). We take the three mixing angles θ_{13}, θ_{12}, and θ_{23} as inputs. With these at hand, Eq. (43) fixes a value of the CP phase δ. Using these and the experimentally determined solar mass splitting, one can calculate from Eq. (44) the combination $m_1^{(0)}m^-$, or equivalently the variable z, which fixes the lightest neutrino mass m_0. It might appear that arbitrarily large values of m_0, and hence $m_1^{(0)}m^-$, may be admitted by taking $\cos\delta$ to smaller and smaller values. However, this is not the case. Experimental data require $\omega=(\pi/4-\theta_{23})$ to lie within determined limits. Since all other factors have experimentally allowed ranges, Eq. (43) also gives lower and upper bounds on δ. Consequently, for any mixing pattern, m_0 lies within a fixed range.

In the left (right) panel of Fig. 2, we show the mixing angle θ_{23} (the CP phase δ) as a function of the lightest neutrino mass m_0 as obtained from this model for different mixing patterns when the best-fit values of the various measured angles and mass splittings are used. The NSM, BM, TBM, and GR correspond to the green solid, pink dashed, red dot-dashed, and violet dotted curves respectively. The thick (thin) curves of each type indicate normal (inverted) mass orderings. Note that normal and inverted orderings are always associated with the first and second octants of θ_{23} respectively. For normal (inverted) ordering with the NSM mixing pattern, δ lies in the first (second) quadrant, while for the other cases, it is in the second (first) quadrant. As expected, for inverted ordering, $|\delta|$ stays close to $\pi/2$ for the entire range of m_0. For normal ordering, δ is near $\pi/2$ for m_0 larger than around 0.05 eV.

Of course, as indicated in Table V, if δ is a solution for some m_0, then by suitably picking alternate values of the phases $\phi_{1,2}$ which appear in $M_{\nu R}$, one can also get a second solution with the phase $-\delta$. We have not shown this mirror set of solutions in Fig. 2. The T2K [14] and NOVA [15] experiments have presented data which may be taken as a preliminary hint of normal ordering associated with $\delta\sim-\pi/2$. As seen from Fig. 2, this is consistent with our model, with $\delta\sim-\pi/2$ favoring m_0 in the quasidegenerate regime, i.e., $m_0\geq\mathcal{O}(0.05\text{ eV})$, for normal ordering. If this result is confirmed by further analysis, then the model will require neutrino masses to be in a range to which ongoing experiments will be sensitive [16,17].

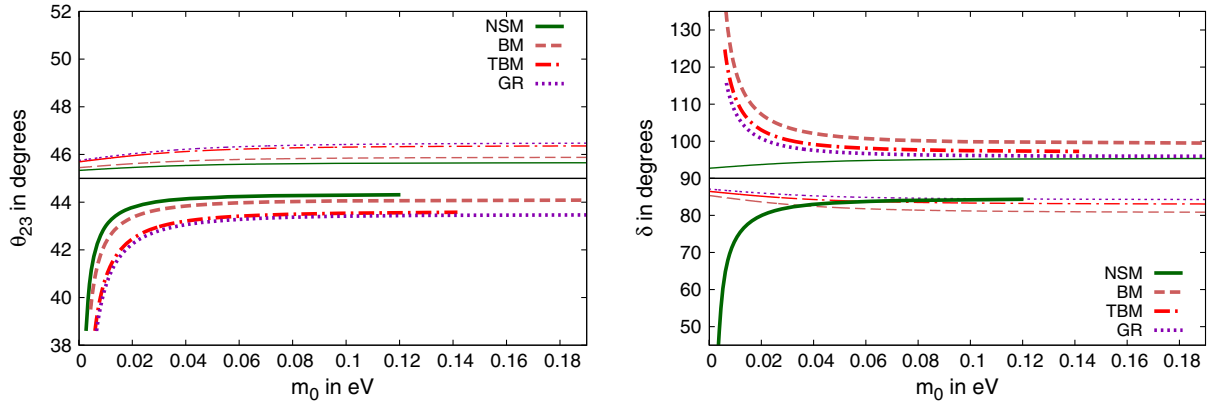

FIG. 2. θ_{23} (left) and the CP phase δ (right) as a function of m_0 from this model for different mixing patterns when the best-fit values of the input data are used. The NSM, BM, TBM, and GR cases correspond to the green solid, pink dashed, red dot-dashed, and violet dotted curves respectively. Thick (thin) curves of each type indicate normal (inverted) mass orderings.

The correlation between the octant of θ_{23}, the quadrant of the CP phase δ, and the ordering of neutrino masses is a smoking-gun signal of this $S_3 \times Z_3$-based model.

IV. CONCLUSIONS

In this paper, we have put forward an $S_3 \times Z_3$ model for neutrino mass and mixing. After assigning the flavor quantum numbers to the leptons and the scalars, we write down the most general Lagrangian consistent with the symmetry. Once the symmetry is broken, the Yukawa couplings give rise to the charged lepton masses as well as the Dirac and Majorana masses for the left- and right-handed neutrinos. Neutrino masses originate from both type-I and type-II seesaw terms of which the former can be treated as a small correction. The dominant type-II seesaw results in the atmospheric mass splitting, no solar splitting, while keeping $\theta_{23} = \pi/4$, and $\theta_{13} = 0$. By a choice of the Yukawa couplings, θ_{12} can be given any preferred value. Thus, at this level, this model can accommodate any of the much-studied tribimaximal, bimaximal, golden ratio, and "no solar mixing" patterns. The smaller type-I seesaw contribution acting as a perturbation generates the solar mass splitting and nudges the mixing angles to values consistent with the global fits. The octants of θ_{23} are correlated with the neutrino mass ordering—the first (second) octant is allowed for normal (inverted) ordering. The model is testable through its predictions for the CP phase δ and from the relationships between mixing angles and mass splittings that it entails. Further, inverted mass ordering is correlated with a near-maximal CP phase δ, and arbitrarily small neutrino masses are permitted. For normal mass ordering, δ can vary over a wider range, and maximality is realized in the quasidegenerate limit. The lightest neutrino mass must be at least a few meV in this case.

ACKNOWLEDGMENTS

S. P. acknowledges support from CSIR, India. A. R. is partially funded by SERB Grant No. SR/S2/JCB-14/2009.

APPENDIX A: ESSENTIALS OF THE S_3 GROUP

S_3 is a discrete group of order 6 which consists of all permutations of three objects. It can be generated by two elements A and B satisfying $A^2 = I = B^3$ and $(AB)(AB) = I$. The group table is given in Table VI.

The group has two one-dimensional representations denoted by 1 and $1'$ and a two-dimensional representation. 1 is inert under the group, while $1'$ changes sign under the action of A. For the two-dimensional representation, a suitable choice of matrices with the specified properties can be readily obtained. We choose

$$I = \begin{pmatrix} 1 & 0 \\ 0 & 1 \end{pmatrix}, \quad A = \begin{pmatrix} 0 & 1 \\ 1 & 0 \end{pmatrix}, \quad B = \begin{pmatrix} \omega & 0 \\ 0 & \omega^2 \end{pmatrix}, \tag{A1}$$

where ω is a cube root of unity, i.e., $\omega = e^{2\pi i/3}$. For this choice of A and B, the remaining matrices of the representation are

$$C = \begin{pmatrix} 0 & \omega^2 \\ \omega & 0 \end{pmatrix}, \quad D = \begin{pmatrix} 0 & \omega \\ \omega^2 & 0 \end{pmatrix}, \quad F = \begin{pmatrix} \omega^2 & 0 \\ 0 & \omega \end{pmatrix}. \tag{A2}$$

The product rules for the different representations are

$$1 \times 1' = 1', \quad 1' \times 1' = 1, \text{ and } 2 \times 2 = 2 + 1 + 1'. \tag{A3}$$

One can see that each of the 2×2 matrices M_{ij} in Eqs. (A1) and (A2) satisfies

$$\sum_{j,l=1,2} \alpha_{jl} M_{ij} M_{kl} = \alpha_{ik}, \tag{A4}$$

where $\alpha_{ij} = 0$ for $i = j$ and $\alpha_{ij} = 1$ for $i \neq j$.

If $\Phi \equiv \binom{\phi_1}{\phi_2}$ and $\Psi \equiv \binom{\psi_1}{\psi_2}$ are two field multiplets transforming under S_3 as doublets, then using Eqs. (A1) and (A4),

$$\phi_1\psi_2 + \phi_2\psi_1 \equiv 1, \qquad \phi_1\psi_2 - \phi_2\psi_1 \equiv 1' \quad \text{and} \quad \begin{pmatrix} \phi_2\psi_2 \\ \phi_1\psi_1 \end{pmatrix} \equiv 2. \tag{A5}$$

Sometimes, we have to deal with Hermitian conjugate fields. Noting the nature of the complex representation [see, for example, B in Eq. (A1)], the conjugate S_3 doublet is $\Phi^\dagger \equiv \binom{\phi_2^\dagger}{\phi_1^\dagger}$. As a result, one has in place of (A5)

$$\phi_2^\dagger\psi_2 + \phi_1^\dagger\psi_1 \equiv 1, \qquad \phi_2^\dagger\psi_2 - \phi_1^\dagger\psi_1 \equiv 1' \quad \text{and} \quad \begin{pmatrix} \phi_1^\dagger\psi_2 \\ \phi_2^\dagger\psi_1 \end{pmatrix} \equiv 2. \tag{A6}$$

Equations (A5) and (A6) are essential in writing down the fermion mass matrices in Sec. II.

APPENDIX B: THE SCALAR POTENTIAL AND ITS MINIMUM

As seen in Table III, this model has a rich scalar field content. In this Appendix, we write down the scalar potential of the model, keeping all these fields, and derive conditions which must be met by the coefficients of the various terms so that the desired vevs can be achieved. These conditions ensure that the potential is locally minimized by this choice.

Table III displays the behavior of the scalar fields under $S_3 \times Z_3$ besides the gauged electroweak $SU(2)_L \times U(1)_Y$. The fields also carry a lepton number. The scalar potential

is the most general polynomial in these fields with up to quartic terms. Our first step will be to write down the explicit form of this potential. Here, we do not exclude any term permitted by the symmetries. $SU(2)_L \times U(1)_Y$ invariance of the terms as well as the Abelian lepton number and Z_3 conservation are readily verified. It is only the S_3 behavior which merits special attention.

There are a variety of scalar fields in this model, e.g., $SU(2)_L$ singlets, doublets, and triplets. Therefore, the scalar potential has a large number of terms. For simplicity, we choose all couplings in the potential to be real. In this Appendix, we list the potential in separate parts: (a) those belonging to any one $SU(2)_L$ sector and (b) intersector couplings of scalars. The $SU(2)_L$ singlet vevs, which are responsible for the right-handed neutrino mass, are significantly larger than those of other scalars. So, in the second category, we retain only those terms which couple the singlet fields to either the doublet or the triplet sectors.

1. $SU(2)_L$ singlet sector

The $SU(2)_L$ singlet sector comprises of two fields χ and γ transforming as $1(\omega)$ and $1'(\omega)$ of $S_3(Z_3)$ respectively. They have $L = 0$. The scalar potential arising out of these is

$$V_{\text{singlet}} = m_\chi^2 \chi^\dagger \chi + m_\gamma^2 \gamma^\dagger \gamma + \Lambda_1^s \{\gamma^2 \chi + \text{h.c.}\} + \frac{\lambda_1^s}{2}[\chi^\dagger \chi]^2 + \frac{\lambda_2^s}{2}[\gamma^\dagger \gamma]^2 + \frac{\lambda_3^s}{2}(\chi^\dagger \chi)(\gamma^\dagger \gamma) + \lambda_4^s\{(\gamma^\dagger \chi)(\gamma^\dagger \chi) + \text{h.c.}\}, \tag{B1}$$

where the coefficient of the cubic term, Λ_1^s, carries the same dimension as mass while the λ_i^s are dimensionless.

2. $SU(2)_L$ doublet sector

The $SU(2)_L$ doublet sector of the model has two fields $\Phi_{a,b}$ that are doublets of S_3, in addition to α, β, and η which are S_3 singlets. Among them, all fields except Φ_b and α ($\in \omega$ of Z_3) are invariant under Z_3.

$$\begin{aligned} V_{\text{doublet}} = {} & m_{\Phi_a}^2 \Phi_a^\dagger \Phi_a + m_{\Phi_b}^2 \Phi_b^\dagger \Phi_b + m_\eta^2 \eta^\dagger \eta + m_\alpha^2 \alpha^\dagger \alpha + m_\beta^2 \beta^\dagger \beta + \frac{\lambda_1^d}{2}(\Phi_a^\dagger \Phi_a)^2 + \frac{\lambda_2^d}{2}(\Phi_b^\dagger \Phi_b)^2 + \frac{\lambda_3^d}{2}(\Phi_a^\dagger \Phi_a)(\Phi_b^\dagger \Phi_b) \\ & + \frac{\lambda_4^d}{2}(\Phi_a^\dagger \Phi_b)(\Phi_b^\dagger \Phi_a) + \frac{\lambda_5^d}{2}(\Phi_a^\dagger \Phi_a)(\eta^\dagger \eta) + \frac{\lambda_6^d}{2}(\Phi_a^\dagger \Phi_a)(\alpha^\dagger \alpha) + \frac{\lambda_7^d}{2}(\Phi_a^\dagger \Phi_a)(\beta^\dagger \beta) + \frac{\lambda_8^d}{2}(\Phi_b^\dagger \Phi_b)(\alpha^\dagger \alpha) \\ & + \frac{\lambda_9^d}{2}(\Phi_b^\dagger \Phi_b)(\beta^\dagger \beta) + \frac{\lambda_{10}^d}{2}(\Phi_b^\dagger \Phi_b)(\eta^\dagger \eta) + \frac{\lambda_{11}^d}{2}(\alpha^\dagger \alpha)^2 + \frac{\lambda_{12}^d}{2}(\alpha^\dagger \alpha)(\eta^\dagger \eta) + \frac{\lambda_{13}^d}{2}(\alpha^\dagger \eta)(\eta^\dagger \alpha) \\ & + \frac{\lambda_{14}^d}{2}(\alpha^\dagger \alpha)(\beta^\dagger \beta) + \frac{\lambda_{15}^d}{2}(\eta^\dagger \eta)^2 + \frac{\lambda_{16}^d}{2}(\eta^\dagger \eta)(\beta^\dagger \beta) + \lambda_{17}^d\{(\Phi_a^\dagger \Phi_b)(\alpha^\dagger \eta) + \text{h.c.}\} + \frac{\lambda_{18}^d}{2}(\beta^\dagger \beta)^2. \end{aligned} \tag{B2}$$

Leaving aside S_3 properties for the moment, to which we return below, out of any $SU(2)$ doublet Φ, one can construct two quartic invariants $(\Phi^\dagger \Phi)(\Phi^\dagger \Phi)$ and $(\Phi^\dagger \vec{\tau} \Phi)(\Phi^\dagger \vec{\tau} \Phi)$. Needless to say, this can be generalized to the case where several distinct $SU(2)$ doublets are involved. In order to avoid cluttering, in Eq. (B2), we have displayed only the first combination for all quartic terms.

The quartic terms involving λ_1 to λ_4 in Eq. (B2) are combinations of two pairs of S_3 doublets. Each pair can combine in accordance with $2 \times 2 = 1 + 1' + 2$ resulting in three terms. The S_3 invariant in the potential arises from a combination of the 1, 1′, or 2 from one pair with the corresponding term from the other pair. Thus, for each such term of four S_3 doublets, three possible singlet combinations exist [recall, Eq. (A3)], and we have to keep an account of all of them. We elaborate on this using as an example the λ_1^d term which actually stands for a set of terms:

$$\frac{\lambda_1^d}{2}(\Phi_a^\dagger \Phi_a)^2 \to \lambda_{1_1}^d[(\Phi_1^\dagger \Phi_1) + (\Phi_2^\dagger \Phi_2)]^2 + \lambda_{1_{1'}}^d[(\Phi_1^\dagger \Phi_1) - (\Phi_2^\dagger \Phi_2)]^2 + \lambda_{1_2}^d[(\Phi_1^\dagger \Phi_2)(\Phi_2^\dagger \Phi_1) + (\Phi_2^\dagger \Phi_1)(\Phi_1^\dagger \Phi_2)]. \tag{B3}$$

Substituting vevs, $\langle \Phi_1 \rangle = v_1$, and $\langle \Phi_2 \rangle = v_2$ and defining $\lambda_{1_1}^d + \lambda_{1_{1'}}^d = \frac{\lambda_{a_1}^d}{2}$, and $2(\lambda_{1_1}^d - \lambda_{1_{1'}}^d + \lambda_{1_2}^d) = \frac{\lambda_{a_2}^d}{2}$, we get

$$\frac{\lambda_1^d}{2}(\Phi_a^\dagger \Phi_a)^2 \longrightarrow \frac{\lambda_{a_1}^d}{2}[(v_1^* v_1)^2 + (v_2^* v_2)^2] + \frac{\lambda_{a_2}^d}{2}(v_1^* v_1)(v_2^* v_2). \tag{B4}$$

Similarly,

$$\frac{\lambda_2^d}{2}(\Phi_b^\dagger\Phi_b)^2 \longrightarrow \frac{\lambda_{b_1}^d}{2}[(v_3^*v_3)^2+(v_4^*v_4)^2]+\frac{\lambda_{b_2}^d}{2}(v_3^*v_3)(v_4^*v_4), \tag{B5}$$

where $\langle\Phi_3\rangle = v_3$ and $\langle\Phi_4\rangle = v_4$. Further,

$$\begin{aligned}\frac{\lambda_3^d}{2}[(\Phi_a^\dagger\Phi_a)(\Phi_b^\dagger\Phi_b)] \to{}& \lambda_{3_1}^d[(\Phi_1^\dagger\Phi_1+\Phi_2^\dagger\Phi_2)(\Phi_3^\dagger\Phi_3+\Phi_4^\dagger\Phi_4)]+\lambda_{3_{1'}}^d[(\Phi_1^\dagger\Phi_1-\Phi_2^\dagger\Phi_2)(\Phi_3^\dagger\Phi_3-\Phi_4^\dagger\Phi_4)]\\ &+\lambda_{3_2}^d[(\Phi_1^\dagger\Phi_2)(\Phi_4^\dagger\Phi_3)+(\Phi_2^\dagger\Phi_1)(\Phi_3^\dagger\Phi_4)].\end{aligned} \tag{B6}$$

Substituting the respective vevs and defining $\lambda_{3_1}^d+\lambda_{3_{1'}}^d=\frac{\lambda_{ab_1}^d}{2}$, $\lambda_{3_1}^d-\lambda_{3_{1'}}^d=\frac{\lambda_{ab_2}^d}{2}$, and $\lambda_{3_2}^d=\lambda_{ab_3}^d$, we get

$$\begin{aligned}\frac{\lambda_3^d}{2}[(\Phi_a^\dagger\Phi_a)(\Phi_b^\dagger\Phi_b)] \longrightarrow{}& \frac{\lambda_{ab_1}^d}{2}[(v_1^*v_1)(v_3^*v_3)+(v_2^*v_2)(v_4^*v_4)]+\frac{\lambda_{ab_2}^d}{2}[(v_1^*v_1)(v_4^*v_4)+(v_2^*v_2)(v_3^*v_3)]\\ &+\lambda_{ab_3}^d[(v_1^*v_2)(v_4^*v_3)+(v_2^*v_1)(v_3^*v_4)].\end{aligned} \tag{B7}$$

In a similar fashion, the λ_4^d term when expanded will lead to

$$\begin{aligned}\frac{\lambda_4^d}{2}[(\Phi_a^\dagger\Phi_b)(\Phi_b^\dagger\Phi_a)] \longrightarrow{}& \frac{\tilde\lambda_{ab_1}^d}{2}[(v_1^*v_3)(v_3^*v_1)+(v_2^*v_4)(v_4^*v_2)]+\frac{\tilde\lambda_{ab_2}^d}{2}[(v_1^*v_3)(v_4^*v_2)+(v_2^*v_4)(v_3^*v_1)]\\ &+\tilde\lambda_{ab_3}^d[(v_1^*v_4)(v_4^*v_1)+(v_2^*v_3)(v_3^*v_2)].\end{aligned} \tag{B8}$$

Adding Eqs. (B7) and (B8), we get

$$\begin{aligned}\frac{\lambda_3^d}{2}[(\Phi_a^\dagger\Phi_a)(\Phi_b^\dagger\Phi_b)]+\frac{\lambda_4^d}{2}[(\Phi_a^\dagger\Phi_b)(\Phi_b^\dagger\Phi_a)] ={}& \frac{\hat\lambda_{ab_1}^d}{2}[(v_1^*v_1)(v_3^*v_3)+(v_2^*v_2)(v_4^*v_4)]+\frac{\hat\lambda_{ab_2}^d}{2}[(v_1^*v_1)(v_4^*v_4)+(v_2^*v_2)(v_3^*v_3)]\\ &+\hat\lambda_{ab_3}^d[(v_1^*v_2)(v_4^*v_3)+(v_2^*v_1)(v_3^*v_4)],\end{aligned} \tag{B9}$$

where $\frac{\hat\lambda_{ab_1}^d}{2}\equiv\frac{\tilde\lambda_{ab_1}^d}{2}+\frac{\lambda_{ab_1}^d}{2}$, $\frac{\hat\lambda_{ab_2}^d}{2}\equiv\tilde\lambda_{ab_3}^d+\frac{\lambda_{ab_2}^d}{2}$, and $\hat\lambda_{ab_3}^d\equiv\frac{\tilde\lambda_{ab_2}^d}{2}+\lambda_{ab_3}^d$. Also, summing up the λ_{12}^d and λ_{13}^d terms leads to $\frac{\hat\lambda_{123}^d}{2}(v_\alpha^*v_\alpha)(v_\eta^*v_\eta)$, where $\hat\lambda_{123}^d\equiv\lambda_{12}^d+\lambda_{13}^d$.

3. $SU(2)_L$ triplet sector

Both the $SU(2)_L$ triplets present in our model (Δ_L, ρ_L) that are responsible for Majorana mass generation of the left handed neutrinos happen to be S_3 invariants and differ only in their Z_3 properties, i.e., $\Delta_L(1)$ and $\rho_L(\omega)$.

$$\begin{aligned}V_{\text{triplet}} ={}& m_{\Delta_L}^2\Delta_L^\dagger\Delta_L+m_{\rho_L}^2\rho_L^\dagger\rho_L+\frac{\lambda_1^t}{2}[\Delta_L^\dagger\Delta_L]^2+\frac{\lambda_2^t}{2}[\rho_L^\dagger\rho_L]^2+\frac{\lambda_3^t}{2}(\Delta_L^\dagger\Delta_L)(\rho_L^\dagger\rho_L)\\ &+\frac{\lambda_4^t}{2}(\Delta_L^\dagger\rho_L)(\rho_L^\dagger\Delta_L)+\frac{\lambda_5^t}{2}(\Delta_L\rho_L)(\Delta_L\rho_L)^\dagger.\end{aligned} \tag{B10}$$

It is noteworthy that when we write the minimized potential in terms of the vacuum expectation values the λ_3^t, λ_4^t, and λ_5^t terms will be providing the same contribution as far as potential minimization is concerned. Thus, we can club these couplings together as $\lambda_{345}^t\equiv\lambda_3^t+\lambda_4^t+\lambda_5^t$.

4. Intersector terms

So far, we have listed those terms in the potential which arise from scalars of any specific $SU(2)_L$ behavior—singlets, doublets, or triplets. In addition, there can be terms which couple one of these sectors to another. Since the vacuum expectation values of the singlet scalars are the largest, we only consider here the couplings of this sector to the others. The $SU(2)_L$ triplet sector vev is very small, and we drop the doublet-triplet cross-sector couplings.

a. $SU(2)_L$ singlet-doublet cross-sector

Couplings between the $SU(2)_L$ singlet and doublet scalars in the potential give rise to the terms

$$\begin{aligned}V_{ds} = {} & \Lambda_1^{ds}[(\Phi_b^\dagger \Phi_a)_{1'}\gamma + \text{h.c.}] + \Lambda_2^{ds}[(\Phi_b^\dagger \Phi_a)_1 \chi + \text{h.c.}] + \Lambda_3^{ds}[(\alpha^\dagger \eta)\chi + \text{h.c.}] + \frac{\lambda_1^{ds}}{2}(\Phi_a^\dagger \Phi_a)(\chi^\dagger \chi) + \frac{\lambda_2^{ds}}{2}(\Phi_a^\dagger \Phi_a)(\gamma^\dagger \gamma) \\ & + \frac{\lambda_3^{ds}}{2}(\Phi_b^\dagger \Phi_b)(\chi^\dagger \chi) + \frac{\lambda_4^{ds}}{2}(\Phi_b^\dagger \Phi_b)(\gamma^\dagger \gamma) + \frac{\lambda_5^{ds}}{2}(\alpha^\dagger \alpha)(\chi^\dagger \chi) + \frac{\lambda_6^{ds}}{2}(\alpha^\dagger \alpha)(\gamma^\dagger \gamma) + \frac{\lambda_7^{ds}}{2}(\eta^\dagger \eta)(\chi^\dagger \chi) + \frac{\lambda_8^{ds}}{2}(\eta^\dagger \eta)(\gamma^\dagger \gamma) \\ & + \lambda_9^{ds}[(\Phi_a^\dagger \Phi_b)\chi^2 + \text{h.c.}] + \lambda_{10}^{ds}[(\Phi_a^\dagger \Phi_b)\gamma^2 + \text{h.c.}] + \lambda_{11}^{ds}[(\eta^\dagger \alpha)\chi^2 + \text{h.c.}] + \lambda_{12}^{ds}[(\eta^\dagger \alpha)\gamma^2 + \text{h.c.}] \\ & + \lambda_{13}^{ds}[(\Phi_a^\dagger \Phi_b)_{1'}(\chi\gamma) + \text{h.c.}] + \frac{\lambda_{14}^{ds}}{2}(\beta^\dagger \beta)(\chi^\dagger \chi) + \frac{\lambda_{15}^{ds}}{2}(\beta^\dagger \beta)(\gamma^\dagger \gamma). \end{aligned} \tag{B11}$$

b. $SU(2)_L$ singlet-triplet cross-sector

The terms in the potential which arise from couplings between the $SU(2)_L$ singlet and triplet scalars are

$$\begin{aligned}V_{ts} = {} & \Lambda_1^{ts}[(\rho_L^\dagger \Delta_L)\chi + \text{h.c.}] + \frac{\lambda_1^{ts}}{2}(\Delta_L^\dagger \Delta_L)(\chi^\dagger \chi) \\ & + \frac{\lambda_2^{ts}}{2}(\Delta_L^\dagger \Delta_L)(\gamma^\dagger \gamma) + \frac{\lambda_3^{ts}}{2}(\rho_L^\dagger \rho_L)(\chi^\dagger \chi) \\ & + \frac{\lambda_4^{ts}}{2}(\rho_L^\dagger \rho_L)(\gamma^\dagger \gamma) + \lambda_5^{ts}\{(\Delta_L^\dagger \rho_L)\chi^2 + \text{h.c.}\} \\ & + \lambda_6^{ts}\{(\Delta_L^\dagger \rho_L)\gamma^2 + \text{h.c.}\}. \end{aligned} \tag{B12}$$

5. Minimization conditions

The vevs of the scalar fields are given in Table III. Using these,

$SU(2)_L$ singlets: $\langle \gamma^0 \rangle = u_\gamma$ and $\langle \chi^0 \rangle = u_\chi$.
$SU(2)_L$ doublets:

$$\langle \Phi_a \rangle = \begin{pmatrix} 0 & v_1 \\ 0 & v_2 \end{pmatrix},$$

$$\langle \Phi_b \rangle = \begin{pmatrix} 0 & v_3 \\ 0 & v_4 \end{pmatrix},$$

$\langle \eta \rangle = v_\eta(0 \quad 1)$, $\langle \alpha \rangle = v_\alpha(0 \quad 1)$ and $\langle \beta \rangle = v_\beta(1 \quad 0)$.

Recall that from the structure of the charged lepton mass matrix Eq. (13) requires $v_2/v_1 = v_4/v_3 = A$ where the real quantity $A = m_\mu/m_\tau$. We often also need $B \equiv (1 + A^2)$.

$SU(2)_L$ triplets: $\langle \rho_L^0 \rangle = v_\rho$ and $\langle \Delta_L^0 \rangle = v_\Delta$.

a. $SU(2)_L$ singlet sector

$$\frac{\partial V_{\text{singlet}}|_{\min}}{\partial u_\chi^*} = 0 \Rightarrow u_\chi[m_\chi^2 + \lambda_1^s u_\chi^* u_\chi] + \Lambda_1^s (u_\gamma^*)^2 + u_\gamma\left[\frac{\lambda_3^s}{2} u_\chi u_\gamma^* + 2\lambda_4^s u_\chi^* u_\gamma\right] = 0, \tag{B13}$$

and

$$\frac{\partial V_{\text{singlet}}|_{\min}}{\partial u_\gamma^*} = 0 \Rightarrow u_\gamma[m_\gamma^2 + \lambda_2^s u_\gamma^* u_\gamma] + 2\Lambda_1^s (u_\gamma^* u_\chi^*) + u_\chi\left[\frac{\lambda_3^s}{2} u_\gamma u_\chi^* + 2\lambda_4^s u_\gamma^* u_\chi\right] = 0. \tag{B14}$$

b. $SU(2)_L$ doublet sector

Define $V_{\mathcal{D}} = V_{\text{doublet}} + V_{ds}$:

$$\begin{aligned}\frac{\partial V_{\mathcal{D}}|_{\min}}{\partial v_\alpha^*} = {} & v_\alpha\left[m_\alpha^2 + \frac{\lambda_6^d}{2}(v_1^* v_1)B + \frac{\lambda_8^d}{2}(v_3^* v_3)B + \lambda_{11}^d (v_\alpha^* v_\alpha) + \frac{\hat{\lambda}_{123}^d}{2}(v_\eta^* v_\eta) + \lambda_{14}^d (v_\beta^* v_\beta)\right] \\ & + v_\alpha\left[\frac{\lambda_5^{ds}}{2}(u_\chi^* u_\chi) + \frac{\lambda_6^{ds}}{2}(u_\gamma^* u_\gamma)\right] + v_\eta[\lambda_{17}^d (v_1^* v_3)B + \Lambda_3^{ds} u_\chi + \lambda_{11}^{ds}(u_\chi^*)^2 + \lambda_{12}^{ds}(u_\gamma^*)^2] = 0, \end{aligned} \tag{B15}$$

$$\frac{\partial V_{\mathcal{D}}|_{\min}}{\partial v_\beta^*} = v_\beta\left[m_\beta^2 + \frac{\lambda_7^d}{2}(v_1^* v_1)B + \frac{\lambda_9^d}{2}(v_3^* v_3)B + \frac{\lambda_{14}^d}{2}(v_\alpha^* v_\alpha) + \frac{\lambda_{16}^d}{2}(v_\eta^* v_\eta) + \lambda_{18}^d(v_\beta^* v_\beta)\right] + v_\beta\left[\frac{\lambda_{14}^{ds}}{2}(u_\chi^* u_\chi) + \frac{\lambda_{15}^{ds}}{2}(u_\gamma^* u_\gamma)\right] = 0, \tag{B16}$$

$$\frac{\partial V_{\mathcal{D}}|_{\min}}{\partial v_\eta^*} = v_\eta\left[m_\eta^2 + \frac{\lambda_5^d}{2}(v_1^* v_1)B + \frac{\lambda_{10}^d}{2}(v_3^* v_3)B + \frac{\hat{\lambda}_{123}^d}{2}(v_\alpha^* v_\alpha) + \lambda_{15}^d(v_\eta^* v_\eta) + \frac{\lambda_{16}^d}{2}(v_\beta^* v_\beta)\right] + v_\eta\left[\frac{\lambda_7^{ds}}{2}(u_\chi^* u_\chi) + \frac{\lambda_8^{ds}}{2}(u_\gamma^* u_\gamma)\right]$$
$$+ v_\alpha[\lambda_{17}^d(v_3^* v_1)B + \Lambda_3^{ds} u_\chi^* + \lambda_{11}^{ds}(u_\chi)^2 + \lambda_{12}^{ds}(u_\gamma)^2] = 0, \tag{B17}$$

$$\frac{\partial V_{\mathcal{D}}|_{\min}}{\partial v_1^*} = v_1\left[m_{\Phi_a}^2 + (v_1^* v_1)\left(\lambda_{a_1}^d + A^2\frac{\lambda_{a_2}^d}{2}\right) + (v_3^* v_3)\left(\frac{\hat{\lambda}_{ab_1}^d}{2} + A^2\frac{\hat{\lambda}_{ab_2}^d}{2} + A^2\hat{\lambda}_{ab_3}^d\right)\right]$$
$$+ v_1\left[\left\{\frac{\lambda_5^d}{2}(v_\eta^* v_\eta) + \frac{\lambda_6^d}{2}(v_\alpha^* v_\alpha) + \frac{\lambda_7^d}{2}(v_\beta^* v_\beta)\right\} + \left\{\frac{\lambda_1^{ds}}{2}(u_\chi^* u_\chi) + \frac{\lambda_2^{ds}}{2}(u_\gamma^* u_\gamma)\right\}\right]$$
$$+ v_3[\{\lambda_{17}^d(v_\alpha^* v_\eta)\} + \{\Lambda_1^{ds} u_\gamma^* + \Lambda_2^{ds} u_\chi^* + \lambda_9^{ds}(u_\chi)^2 + \lambda_{10}^{ds}(u_\gamma)^2 + \lambda_{13}^{ds}(u_\chi u_\gamma)\}] = 0, \tag{B18}$$

$$\frac{\partial V_{\mathcal{D}}|_{\min}}{\partial v_2^*} = Av_1\left[m_{\Phi_a}^2 + (v_1^* v_1)\left(A^2\lambda_{a_1}^d + \frac{\lambda_{a_2}^d}{2}\right) + (v_3^* v_3)\left(A^2\frac{\hat{\lambda}_{ab_1}^d}{2} + \frac{\hat{\lambda}_{ab_2}^d}{2} + \hat{\lambda}_{ab_3}^d\right)\right]$$
$$+ Av_1\left[\left\{\frac{\lambda_5^d}{2}(v_\eta^* v_\eta) + \frac{\lambda_6^d}{2}(v_\alpha^* v_\alpha) + \frac{\lambda_7^d}{2}(v_\beta^* v_\beta)\right\} + \left\{\frac{\lambda_1^{ds}}{2}(u_\chi^* u_\chi) + \frac{\lambda_2^{ds}}{2}(u_\gamma^* u_\gamma)\right\}\right]$$
$$+ Av_3[\{\lambda_{17}^d(v_\alpha^* v_\eta)\} + \{-\Lambda_1^{ds} u_\gamma^* + \Lambda_2^{ds} u_\chi^* + \lambda_9^{ds}(u_\chi)^2 + \lambda_{10}^{ds}(u_\gamma)^2 - \lambda_{13}^{ds}(u_\chi u_\gamma)\}] = 0, \tag{B19}$$

$$\frac{\partial V_{\mathcal{D}}|_{\min}}{\partial v_3^*} = v_3\left[m_{\Phi_b}^2 + (v_3^* v_3)\left(\lambda_{b_1}^d + A^2\frac{\lambda_{b_2}^d}{2}\right) + (v_1^* v_1)\left(\frac{\hat{\lambda}_{ab_1}^d}{2} + A^2\frac{\hat{\lambda}_{ab_2}^d}{2} + A^2\hat{\lambda}_{ab_3}^d\right)\right]$$
$$+ v_3\left[\left\{\frac{\lambda_8^d}{2}(v_\alpha^* v_\alpha) + \frac{\lambda_9^d}{2}(v_\beta^* v_\beta) + \frac{\lambda_{10}^d}{2}(v_\eta^* v_\eta)\right\} + \left\{\frac{\lambda_3^{ds}}{2}(u_\chi^* u_\chi) + \frac{\lambda_4^{ds}}{2}(u_\gamma^* u_\gamma)\right\}\right]$$
$$+ v_1[\{\lambda_{17}^d(v_\eta^* v_\alpha)\} + \{\Lambda_1^{ds} u_\gamma + \Lambda_2^{ds} u_\chi + \lambda_9^{ds}(u_\chi^*)^2 + \lambda_{10}^{ds}(u_\gamma^*)^2 + \lambda_{13}^{ds}(u_\chi^* u_\gamma^*)\}] = 0, \tag{B20}$$

$$\frac{\partial V_{\mathcal{D}}|_{\min}}{\partial v_4^*} = Av_3\left[m_{\Phi_b}^2 + (v_3^* v_3)\left(A^2\lambda_{b_1}^d + \frac{\lambda_{b_2}^d}{2}\right) + (v_1^* v_1)\left(A^2\frac{\hat{\lambda}_{ab_1}^d}{2} + \frac{\hat{\lambda}_{ab_2}^d}{2} + \hat{\lambda}_{ab_3}^d\right)\right]$$
$$+ Av_3\left[\left\{\frac{\lambda_8^d}{2}(v_\alpha^* v_\alpha) + \frac{\lambda_9^d}{2}(v_\beta^* v_\beta) + \frac{\lambda_{10}^d}{2}(v_\eta^* v_\eta)\right\} + \left\{\frac{\lambda_3^{ds}}{2}(u_\chi^* u_\chi) + \frac{\lambda_4^{ds}}{2}(u_\gamma^* u_\gamma)\right\}\right]$$
$$+ Av_1[\{\lambda_{17}^d(v_\eta^* v_\alpha)\} + \{-\Lambda_1^{ds} u_\gamma + \Lambda_2^{ds} u_\chi + \lambda_9^{ds}(u_\chi^*)^2 + \lambda_{10}^{ds}(u_\gamma^*)^2 - \lambda_{13}^{ds}(u_\chi^* u_\gamma^*)\}] = 0. \tag{B21}$$

c. $SU(2)_L$ triplet sector

Define $V_{\mathcal{T}} = V_{\text{triplet}} + V_{ts}$:

$$\frac{\partial V_{\mathcal{T}}|_{\min}}{\partial v_\Delta^*} = v_\Delta\left[\left\{m_{\Delta_L}^2 + \lambda_1^t(v_\Delta^* v_\Delta) + \frac{\lambda_{345}^t}{2}(v_\rho^* v_\rho)\right\} + \left\{\frac{\lambda_1^{ts}}{2}(u_\chi^* u_\chi) + \frac{\lambda_2^{ts}}{2}(u_\gamma^* u_\gamma)\right\}\right] + v_\rho[\Lambda_1^{ts} u_\chi^* + \lambda_5^{ts} u_\chi^2 + \lambda_6^{ts} u_\gamma^2] = 0, \tag{B22}$$

$$\frac{\partial V_{\mathcal{T}}|_{\min}}{\partial v_\rho^*} = v_\rho\left[\left\{m_{\rho_L}^2 + \lambda_2^t(v_\rho^* v_\rho) + \frac{\lambda_{345}^t}{2}(v_\Delta^* v_\Delta)\right\} + \left\{\frac{\lambda_3^{ts}}{2}(u_\chi^* u_\chi) + \frac{\lambda_4^{ts}}{2}(u_\gamma^* u_\gamma)\right\}\right]$$
$$+ v_\Delta[\Lambda_1^{ts} u_\chi + \lambda_5^{ts}(u_\chi^*)^2 + \lambda_6^{ts}(u_\gamma^*)^2] = 0. \tag{B23}$$

[1] See, for example, P. F. Harrison and W. G. Scott, Phys. Lett. B **557**, 76 (2003).

[2] S. L. Chen, M. Frigerio, and E. Ma, Phys. Rev. D **70**, 073008 (2004); **70**, 079905(E) (2004); E. Ma, Phys. Rev. D **61**, 033012 (2000).

[3] A sampling is W. Grimus and L. Lavoura, J. High Energy Phys. 08 (2005) 013; R. Jora, J. Schechter, and M. Naeem Shahid, Phys. Rev. D **80**, 093007 (2009); **82**, 079902(E) (2010); Z. z. Xing, D. Yang, and S. Zhou, Phys. Lett. B **690**, 304 (2010); T. Teshima and Y. Okumura, Phys. Rev. D **84**, 016003 (2011); S. Dev, S. Gupta, and R. R. Gautam, Phys. Lett. B **702**, 28 (2011); S. Zhou, Phys. Lett. B **704**, 291 (2011); R. Jora, J. Schechter, and M. N. Shahid, Int. J. Mod. Phys. A **28**, 1350028 (2013); H. B. Benaoum, Phys. Rev. D **87**, 073010 (2013).

[4] S. Morisi, arXiv:hep-ph/0605167; M. Tanimoto and T. Yanagida, Phys. Lett. B **633**, 567 (2006); S. Gupta, C. S. Kim, and P. Sharma, Phys. Lett. B **740**, 353 (2015).

[5] A. E. C. Hernandez, E. C. Mur, and R. Martinez, Phys. Rev. D **90**, 073001 (2014); V. V. Vien and H. N. Long, Zh. Eksp. Teor. Fiz. **145**, 991 (2014); J. Exp. Theor. Phys. **118**, 869 (2014); E. Ma and R. Srivastava, Phys. Lett. B **741**, 217 (2015); D. Meloni, S. Morisi, and E. Peinado, J. Phys. G **38**, 015003 (2011); A. E. Carcamo Hernandez, I. de Medeiros Varzielas, and E. Schumacher, Phys. Rev. D **93**, 016003 (2016); A. E. Carcamo Hernandez, I. de Medeiros Varzielas, and N. A. Neill, Phys. Rev. D **94**, 033011 (2016); D. Das, U. K. Dey, and P. B. Pal, Phys. Lett. B **753**, 315 (2016); R. N. Mohapatra, S. Nasri, and H. B. Yu, Phys. Lett. B **639**, 318 (2006).

[6] F. Feruglio and Y. Lin, Nucl. Phys. **B800**, 77 (2008).

[7] For the present status of θ_{13}, see presentations from Double Chooz, RENO, Daya Bay, and T2K at Neutrino 2016 (http://neutrino2016.iopconfs.org/programme).

[8] S. Pramanick and A. Raychaudhuri, Phys. Rev. D **93**, 033007 (2016).

[9] S. Pramanick and A. Raychaudhuri, Phys. Lett. B **746**, 237 (2015); Int. J. Mod. Phys. A **30**, 1530036 (2015).

[10] B. Brahmachari and A. Raychaudhuri, Phys. Rev. D **86**, 051302 (2012); S. Pramanick and A. Raychaudhuri, Phys. Rev. D **88**, 093009 (2013).

[11] J. Kubo, A. Mondragon, M. Mondragon, and E. Rodriguez-Jauregui, Prog. Theor. Phys. **109**, 795 (2003); **114**, 287(E) (2005); S. Kaneko, H. Sawanaka, T. Shingai, M. Tanimoto, and K. Yoshioka, Prog. Theor. Phys. **117**, 161 (2007).

[12] M. C. Gonzalez-Garcia, M. Maltoni, J. Salvado, and T. Schwetz, J. High Energy Phys. 12 (2012) 123, NuFIT 2.1 (2016).

[13] D. V. Forero, M. Tortola, and J. W. F. Valle, Phys. Rev. D **86**, 073012 (2012).

[14] K. Abe *et al.* (T2K collaboration), Phys. Rev. D **91**, 072010 (2015) (see Fig. 37).

[15] P. Adamson *et al.* (NOVA Collaboration), Phys. Rev. Lett. **116**, 151806 (2016).

[16] M. Haag (KATRIN Collaboration), Proc. Sci., EPS-HEP2013 (**2013**) 518.

[17] See, for example, G. Drexlin, V. Hannen, S. Mertens, and C. Weinheimer, Adv. High Energy Phys. **2013**, 293986 (2013).